Repair of Porcine Articular Cartilage Defect with a Biphasic Osteochondral Composite

Ching-Chuan Jiang,[1] Hongsen Chiang,[1,4] Chun-Jen Liao,[2] Yu-Ju Lin,[2] Tzong-Fu Kuo,[3] Chang-Shun Shieh,[1] Yi-You Huang,[1] Rocky S. Tuan[4]

[1]National Taiwan University Hospital, and National Taiwan University College of Medicine, Taipei, Taiwan

[2]Industry Technology Research Institute, Hsinchu, Taiwan

[3]National Taiwan University Veterinary Hospital, Taipei, Taiwan

[4]Cartilage Biology and Orthopaedics Branch, National Institute of Arthritis, and Musculoskeletal and Skin Diseases, Department of Health and Human Services, National Institutes of Health, 50 South Drive, Building 50/Room 1523, Bethesda, Maryland 20892-8022

Received 9 February 2006; accepted 2 April 2007

Published online 18 June 2007 in Wiley InterScience (www.interscience.wiley.com). DOI 10.1002/jor.20442

ABSTRACT: Autologous chondrocyte implantation (ACI) has been recently used to treat cartilage defects. Partly because of the success of mosaicplasty, a procedure that involves the implantation of native osteochondral plugs, it is of potential significance to consider the application of ACI in the form of biphasic osteochondral composites. To test the clinical applicability of such composite construct, we repaired osteochondral defect with ACI at low cell-seeding density on a biphasic scaffold, and combined graft harvest and implantation in a single surgery. We fabricated a biphasic cylindrical porous plug of DL-poly-lactide-co-glycolide, with its lower body impregnated with β-tricalcium phosphate as the osseous phase. Osteochondral defects were surgically created at the weight-bearing surface of femoral condyles of Lee-Sung mini-pigs. Autologous chondrocytes isolated from the cartilage were seeded into the upper, chondral phase of the plug, which was inserted by press-fitting to fill the defect. Defects treated with cell-free plugs served as control. Outcome of repair was examined 6 months after surgery. In the osseous phase, the biomaterial retained in the center and cancellous bone formed in the periphery, integrating well with native subchondral bone with extensive remodeling, as depicted on X-ray roentgenography by higher radiolucency. In the chondral phase, collagen type II immunohistochemistry and Safranin O histological staining showed hyaline cartilage regeneration in the experimental group, whereas only fibrous tissue formed in the control group. On the International Cartilage Repair Society Scale, the experimental group had higher mean scores in surface, matrix, cell distribution, and cell viability than control, but was comparable with the control group in subchondral bone and mineralization. Tensile stress–relaxation behavior determined by uni-axial indentation test revealed similar creep property between the surface of the experimental specimen and native cartilage, but not the control specimen. Implanted autologous chondrocytes could survive and could yield hyaline-like cartilage in vivo in the biphasic biomaterial construct. Pre-seeding of osteogenic cells did not appear to be necessary to regenerate subchondral bone. © 2007 Orthopaedic Research Society. Published by Wiley Periodicals, Inc.* J Orthop Res 25:1277–1290, 2007

Keywords: autologous chondrocyte implantation; biphasic osteochondral composite

INTRODUCTION

The clinical finding that articular cartilage "once destroyed, is not repaired," has remained unchanged since it was first observed by Hunter in 1743. Full-thickness defect of articular cartilage inevitably progresses to catastrophic arthritis,[1] and no consensus on effective treatment has been achieved thus far. Conventional surgeries, such as abrasive chondroplasty and penetration of subchondral bone, usually rely on stimulation or recruitment of chondrogenic cells, but the outcome is discouraging because of the avascular nature and lack of repair cells in cartilage.[2] Articular cartilage defects have to be repaired, but the supply of graft is severely limiting. Consequently, autologous chondrocyte implantation (ACI) has become a principal procedure in current cell-based cartilage repair.[3,4]

Correspondence to: Rocky S. Tuan (Telephone: 301-451-6854; Fax: 301-435-8017; E-mail: tuanr@mail.nih.gov)

Various modalities of ACI have been introduced to date, including those that involve chondrocytes or chondrogenic cells seeded onto biodegradable scaffolds to generate cartilage constructs in vitro, which in turn are used for implantation.[5–9] Similar to previous trials of patching the cartilage defects with periosteal or perichondrial grafts, these engineered cartilage chips require a technically demanding and time-consuming suture procedure to be fixed onto recipient sites.[10,11] After implantation, inadequate security at the osteochondral junction may lead to dehiscence of cartilage graft from the underlying bone by the shearing force encountered during joint motion. The solution of such problem may be a pre-fashioned osteochondral graft, which is self-secured to the subchondral bone without additional fixation procedure or device, and therefore has good surgical applicability. The clinical success of mosaicplasty using osteochondral grafts[12–15] supports this approach; at the same time, the shortage of donor resources may be overcome by the cell expansion process of ACI. In addition, an osteochondral graft, instead of cartilage alone, may be optimal for the repair of some focal cartilage lesions, such as osteonecrosis and osteochondritis dissecans, that involve both cartilaginous and osseous pathology.

A biphasic scaffold is preferred in constructing such osteochondral graft for both mechanical and biological reasons—a uniform tidemark at the osteochondral junction and integration of the biphasic structure with host tissue to sustain biological function.[16] Such scaffolds should ideally have a rigid osseous phase, to support the overlying cartilage and integrate with the native bone, and a porous chondral phase, to allow the seeding and proliferation of chondrocytes and subsequent deposition of cartilaginous extracellular matrix (ECM).

Most ACI procedures involve the culturing of cells in vitro prior to the secondary implantation surgery. This step is necessary because a cell-seeding density as high as 60×10^6 cells/ml is considered important to produce mechanically sound cartilage.[17] Direct harvest of this number of cells from spared cartilage is at best difficult, if not impossible. However, a recent study indicates that chondrocytes seeded at lower seeding density on selected biomaterial scaffold can synthesize a cartilage-like matrix without prior monolayer expansion.[18] Another possible solution to overcome the short cell resource is an ideal culture environment, which may support the regeneration of cartilage from a limited number of cells. Although sophisticated bioreactors mimicking the intraarticular environment are frequently used to optimize the tissue engineering process, the cartilage defect environment as a "bioactive chamber" provides a more natural setting.[19] If a lower seeding density on suitable scaffold could build cartilage in such ideal environment, an obvious advantage is that cell harvest and implantation steps could both be accomplished in a single surgery. Animal model study is useful in this regard, to test the efficacy of in vivo regeneration of cartilage. Further, animal studies are also critical to verify the clinical applicability of engineered cartilage constructs.[20] As many designs of biphasic osteochondral construct have been introduced in recent years,[16,21–25] it is important to investigate their applicability in living joints.

In this study, we hypothesized that cartilage regeneration in vivo might proceed at a cell density below 5×10^6 cells/ml, so that all procedures for repair of osteochondral defect, including cell harvest, seeding to biphasic scaffold, and construct implantation, could be done in one surgery. In this study, we have developed a biphasic scaffold, and verified its ability to repair osteochondral defects in an animal model with a seed-and-implant surgery.

METHODS

Biomaterials

The biphasic construct was fabricated with a modified solvent merging/particulate leaching method[26] as follows. (1) 1.5 g DL-poly-lactide-co-glycolide (PLGA) particles (molar ratio 85:15, average molecular weight 580,000; Purac, Gorinchem, The Netherlands) and 8.5 g NaCl (Sigma, St. Louis, MO) were dissolved in 40 ml acetone, and the solution was poured into a 10-cm wide, 0.5-cm high cubic Teflon mold. After solvent evaporation, the formed 0.8-mm thick PLGA-NaCl membrane was trimmed to an 8-mm diameter disk and a 25-mm × 5-mm rectangular sheet. (2) PLGA and β-tricalcium phosphate (TCP) (Fluka, Seelze, Germany) of equal weight were dissolved in 40 ml acetone, and NaCl was added to supersaturation. The solution was poured into a Teflon mold, air dried for 48 h, and vacuum dried for 48 h. The resultant PLGA-TCP composite was ground to small particles, and immersed in water overnight to remove the salt; after air drying, 250–440-μm size particles were selected via a 40–60 mesh sieve, and combined with NaCl particles of the same size range, in 15/85 weight ratio. (3) The disk and the sheet prepared in step 1 were assembled onto an 8-mm diameter, 40-mm high cylindrical Teflon mold with a No. 80 stainless steel mesh on the bottom, which was attached to a downward exhaust. The disk was seated on the bottom, and the sheet was wrapped around the inside of the cylinder to make a fillister with the disk. The disk would serve as the chondral phase of the final

construct. Fifty milligrams of NaCl particles were tightly packed centrally on the disk, and the fillister was subsequently tightly filled with 1,000 mg of the PLGA-TCP/NaCl mixture prepared in step 2. Next, 10 ml of 1–4 dioxane solvent (Aldrich Chemical, Milwaukee, WI) was poured into the mold, left to stand for 30 s, and exhausted; 100 ml of methanol was similarly passed through the mold. Finally, the PLGA polymer precipitated and formed a matrix, which was then flushed with abundant water to leach the NaCl particles and remove residual solvent. (4) The fabricated PLGA/PLGA-TCP biphasic construct was removed from the mold and vacuum dried at 0.05 torr for 12 h at room temperature. The final product was a cylindrical plug of 8-mm diameter and 8-mm height (Fig. 1). About 1/6 of the height of the cylinder was PLGA, serving as the chondral phase; the remainder consisted of PLGA-TCP composite, serving as the osseous phase. The overall infrastructure was 85% porosity and 250–400 μm pore dimension. Prepared constructs were immersed in 75% alcohol for 6 h for sterilization, rinsed with phosphate-buffered saline (PBS), vacuum dried, and stored in a desiccator until use.

Experimental Design and Surgical Procedures

Animal experimentation was conducted according to a protocol approved by the Institutional Animal Experiment Committee (National Taiwan University). Ten skeletally mature (7–9 months old) Lee-Sung mini-pigs were used in the experiment, four male and six female. They were housed individually in a sheltered outdoor fenced space with good ventilation, and allowed forage and water ad libitum throughout the experiment. All surgeries were carried out in the operation room of the veterinary hospital with standard surgical routines and sterile techniques.

General anesthesia was induced with intramuscular atropine sulfate (0.03 mg/kg) and Zoletil 50™ (tiletamine/zolazepam, 0.55–0.80 mg/kg, Virbac Laboratories, Carros, France), and maintained by intravenous Citosol (thiamylal, 1.11–1.60 mg/kg, Shinlin-Sinseng Pharmaceutical, Taoyuan, Taiwan). Both knees of each animal were operated at the same surgery, with arthrotomy made through a longitudinal medial parapatellar incision and lateral dislocation of patella. An 8-mm diameter circle was marked by a dermal punch on the center of the distal weight-bearing portion of each femoral condyle. In the right knee, full thickness cartilage was peeled off and retained to isolate chondrocytes, as described later. Each marked area was further drilled to an 8-mm deep cylindrical pit for later repair with either autogenous chondrocyte-seeded construct as experimental group, or blank cell-free construct as control. The two condyles in each knee were assigned alternatively to experimental and control groups, in order to eliminate the effect of side and laterality. Two defects of different animals, one on medial and the other on lateral condyle, were kept empty as the null group, while the other defects were implanted—20 for experimental and 18 for control groups.

After harvesting of autogenous cartilage, the arthrotomy was reduced and closed temporarily with sutures. The animal was kept under anesthesia during the preparation of implants, and the surgery would be continued when the constructs were ready for implantation.

Figure 1. Biphasic cylindrical scaffold ready for cell seeding. About 1.5-mm depth of the top of the cylinder was the soft spongy chondral phase, and the remainder was the more rigid osseous phase. Left, top view; right, side view. (Arrow, chondral phase; bracket, osseous phase).

Graft Processing and Construct Implantation

The harvested cartilage graft was immersed immediately in Dulbecco's modified Eagle's medium (DMEM) (HyClone, Logan, UT) until processing. The graft was processed aseptically: chopped with a scalpel, washed thoroughly with PBS, and digested for 2 h with an enzyme mixture of 0.4% collagenase and 0.1% hyaluronidase (w/w) (Sigma) in DMEM, supplemented with gentamycin and amphotericin B. Tissue debris was removed by filtration through a 40-μm sieve, and chondrocytes in the filtrate were collected with centrifugation at 300*g* for 10 min. Approximately 0.8×10^6 cells were isolated per animal. Cell viability based on Trypan blue exclusion test showed about 90%–95% cell viability. The cells were resuspended in 0.2 ml DMEM and divided evenly into two aliquots. The 0.1-ml aliquot of cell suspension was slowly injected into the chondral phase of a construct with a syringe, so that the spongy biomaterial was fully soaked. The final cell density in the chondral phase of the construct was estimated to be 3×10^6 cells/ml.

At the time of graft implantation, the knee joints were re-opened by removing the sutures, and the prepared biphasic constructs were manually press-fit inserted into the defect such that its surface appeared flush with the articular surface (Fig. 2). The patella was reduced and the wound was closed in layers. The knee joints were not immobilized, and the animal resumed free activity with standing on all their legs as soon as recovery from anesthesia. For 3 postoperative days, Cephalexin 1,000 mg (Glaxovet, Harefield, UK) as antibiotics was injected intramuscularly one dose per day, with intermittent

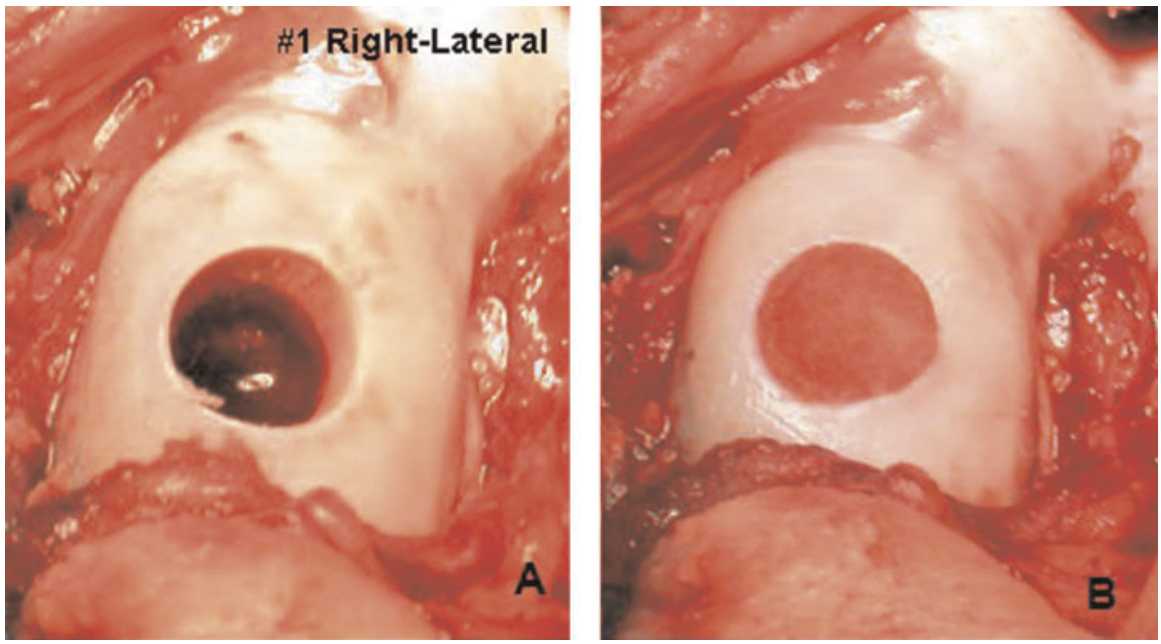

Figure 2. Demonstration of the implantation surgery. (A) Osteochondral defect, 8-mm diameter and 8-mm depth, was created on the distal surface of the condyle by drilling. Marrow seeped from the surrounding cancellous bone and accumulated in the created pit. (B) The biphasic cylindrical plug, either chondrocyte-laden (as shown here) or cell-free, was press-fit inserted into the defect with the surface flush with the articular surface.

analgesic injection of buprenorphine-flunixin. Wound healing was evident at 1 week after surgery.

Examination of Regenerate Tissue

Six months after the transplantation, the animals were euthanized by overdose injection of pentobarbital and the grafted femoral condyles retrieved. Each condyle was inspected for shape and contour, and evaluated X-ray roentgenographically for subchondral bone changes. Each grafted area was bisected along the frontal plane to examine the integration of regenerate tissue with adjacent native tissue. The specimens were then fixed with buffered paraformaldehyde, decalcified overnight in a sodium citrate-formic acid solution, embedded in paraffin, and sectioned for routine hematoxylin and eosin (H&E) staining, Safranin O staining, and immunohistological staining for collagen type II (Chemicon, Temecula, CA).

The regenerate cartilage was scored grossly on a previously developed scale (Table 1),[27] and histologically on the International Cartilage Repair Society (ICRS) Visual Histological Assessment Scale.[20] Two observers, both blind to the treatment, independently scored the specimens. To be defined as hyaline cartilage, the ground substance of the matrix should be homogeneous without fibrous texture with H&E staining, be positively stained for sulfated glycosaminoglycan (sGAG) by Safranin O, and contain predominantly collagen type II, while the cells should be round, exist individually or align in short columns, and sit centrally in lacunae. A cell would be

Table 1. Gross Grading Scale*

Parameter	Grade
Coverage (% area)	
75%–100%	4
50%–75%	3
25%–50%	2
<25%	1
Bare	0
Neocartilage color	
Normal	4
0%–25% abnormal	3
25%–50% abnormal	2
50%–75% abnormal	1
75%–100% abnormal	0
Defect margin (% circumference)	
Invisible	4
0%–25% visible	3
25%–50% visible	2
50%–75% visible	1
75%–100% visible	0
Surface smoothness	
Smooth, flush with adjacent	4
Smooth, raised	3
25%–50% irregular	2
50%–75% irregular	1
75%–100% irregular	0

*Reference.[27]

 DOI 10.1002/jor

considered viable by the presence of a clearly delineated nucleus under H&E staining.[27] All specimens were evaluated on the basis of one parameter at a time. Scores of each individual parameter were analyzed statistically between groups with Wilcoxon rank sum test. Statistical significance of difference was defined at $p < 0.05$.

For biomechanical characterization, the tensile stress–relaxation property of the regenerate and nearby native cartilage were determined by unconfined uni-axial indentation test[28,29] using a custom-designed device. Four randomly selected joints were subjected to testing; each had experimental site on one condyle and control site on the other. Briefly, the thickness of cartilaginous tissue was measured, and the specimen was mounted on an adjustable stage with precise height control. The stage was raised by a predetermined amount to apply a 30% strain on the cartilage surface against a 2-mm diameter bold-tip probe. The reaction force was determined with a stress gauge on the base of the probe, and transformed to compressive stress as a function of time. After the instantaneous peak stress, the specimens were allowed to show a time-dependent creep for 30 min or until equilibrium was reached.

RESULTS

Macroscopic and Histological (ICRS Score) Results

The two sites of null group remained empty defects, whereas all 38 implanted sites were repaired with regenerate tissue. The implanted defects were consistently filled with firm bone, which was covered with fibrous or cartilaginous tissue to varying extents: 11 defects in the experimental group and 4 in the control group had more than 75% area of coverage. The covering tissue in the experimental group consisted of firm, cartilage-like substance in 13 defects, whereas such tissue was found in only 1 defect of the control group. The other specimens of the control group were either covered with soft tissue or bare with exposure of underlying bony tissue (Fig. 3). The experimental group had significantly higher mean scores than control group in all four categories of the Gross Grading Scale.

The biomaterial in the chondral phase was completely resorbed in all implanted constructs. ICRS histological scoring revealed that the experimental group had significantly higher mean scores than the control group in surface morphology, matrix, cell distribution, and cell viability, but both groups were comparable in subchondral bone and cartilage mineralization scores (Fig. 4). The observations are summarized as follows. (1) Surface morphology: Surface smoothness observed histologically roughly paralleled gross observation. In the experimental group, the surface of regenerate cartilage was smooth in 12 specimens, although some of these had visible major fissures. One specimen had a fibrous cap that could be peeled off, revealing the coarse surface of the underlying cartilage tissue. In the control group, the surfaces were generally uneven, but in three specimens, the regenerate fibrocartilage had smooth surface. (2) Matrix: The ground substance of regenerate cartilage in experimental group was homogeneous by H&E staining and contained collagen type II and sGAG, on the basis of positive immunostaining and Safranin O staining, respectively (Fig. 5). In one

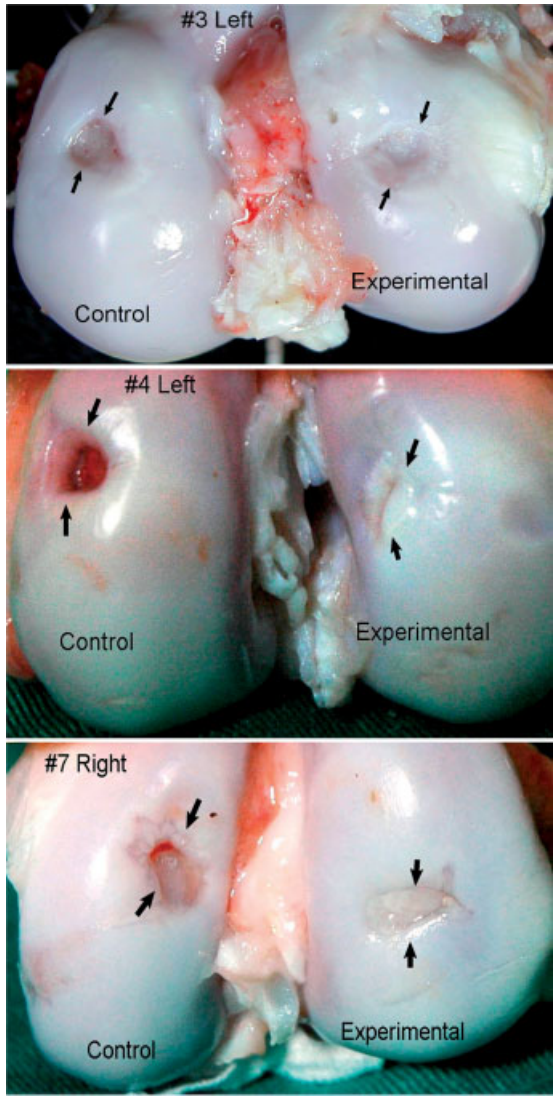

Figure 3. Gross appearance of repaired sites (arrows) at 6 months postoperatively, showing various patterns of tissue regeneration. Three animals are shown here: #3 left, #4 left, and #7 right. In the experimental group, cartilaginous tissue was generated, with various thickness, surface smoothness, and coverage of defects. In control group, cartilaginous tissue was generally absent, and the defects were incompletely filled with bony repair with or without a thin fibrous coverage.

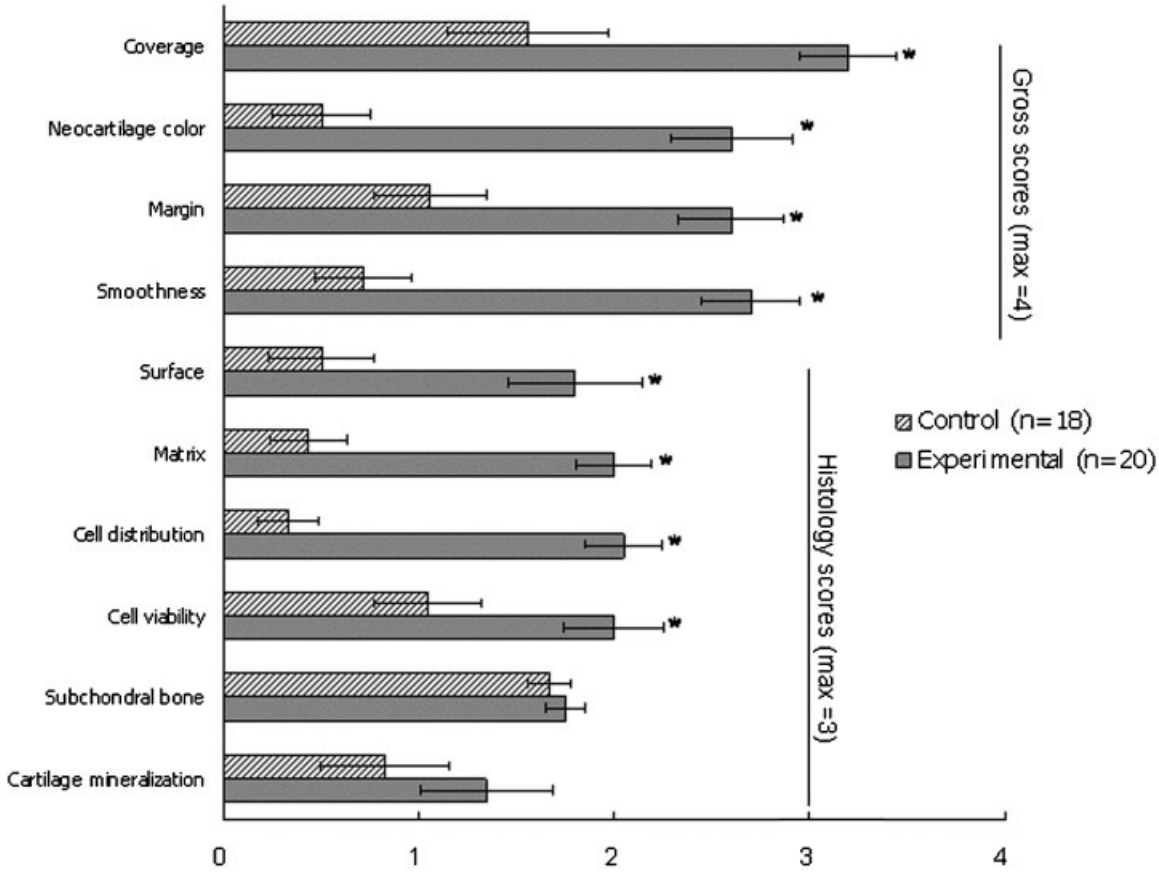

Figure 4. Mean scores of experimental and control groups based on Gross Grading Scale and ICRS histological scale. Asterisks indicate statistically significant difference between groups.

specimen, the hyaline cartilage was capped with tightly adhered fibrous tissue. The regenerative tissue in control group was generally fibrous with darkly H&E -stained coarse streaks. Such fibrocartilage was deficient in collagen type II and sGAG as revealed by specific staining. (3) Cell distribution: As shown in Figure 6, the native cartilage adjacent to the repair sites depicted normal chondrocyte distribution, i.e., cells were located predominantly near the osteochondral junction, in rays of 4–5 within each lacuna, forming a typical palisade architecture. This pattern was not completely rebuilt in the regenerate cartilage of the experimental group. Although also lacunated, the round cells in the regenerate cartilage were distributed more evenly and appeared essentially as individual cells. Short cell columns were found, but were generally oriented randomly rather than perpendicularly to osteochondral junction. Cell clusters or rosettes were also found in three specimens. The lacunated round cell was never found in the control group; instead, individually, spindle-shaped fibroblast-like cells were seen oriented parallel to the osteochondral junction and were packed tightly within intercellular fibers. (4) Cell viability: Viable cells were generally observed in the experimental group. In the control group, the scaffolds were cell-free at the time of implantation; therefore, all cells subsequently found within the scaffolds were considered postoperative immigrant cells. Control group specimens were generally highly hypocellular in their chondral phase, but could be hypercellular in cases where dense fibrous tissues formed. (5) Subchondral bone: In every implanted defect, the osseous space was filled with a complex mixture of unresorbed biomaterial with massive cellular infiltration, and scattered callus and granulation tissue. Cellular reaction was most active peripherally along the junction with native bone, featuring many multinuclear cells (see detailed description below). (6) Mineralization: Regardless of the nature of the regenerate tissue, chondral phase of all specimens showed associated mineralization, as buds of subchondral bone rising beyond the tidemark, and/or as isolated bone islands. Mineralization

 DOI 10.1002/jor

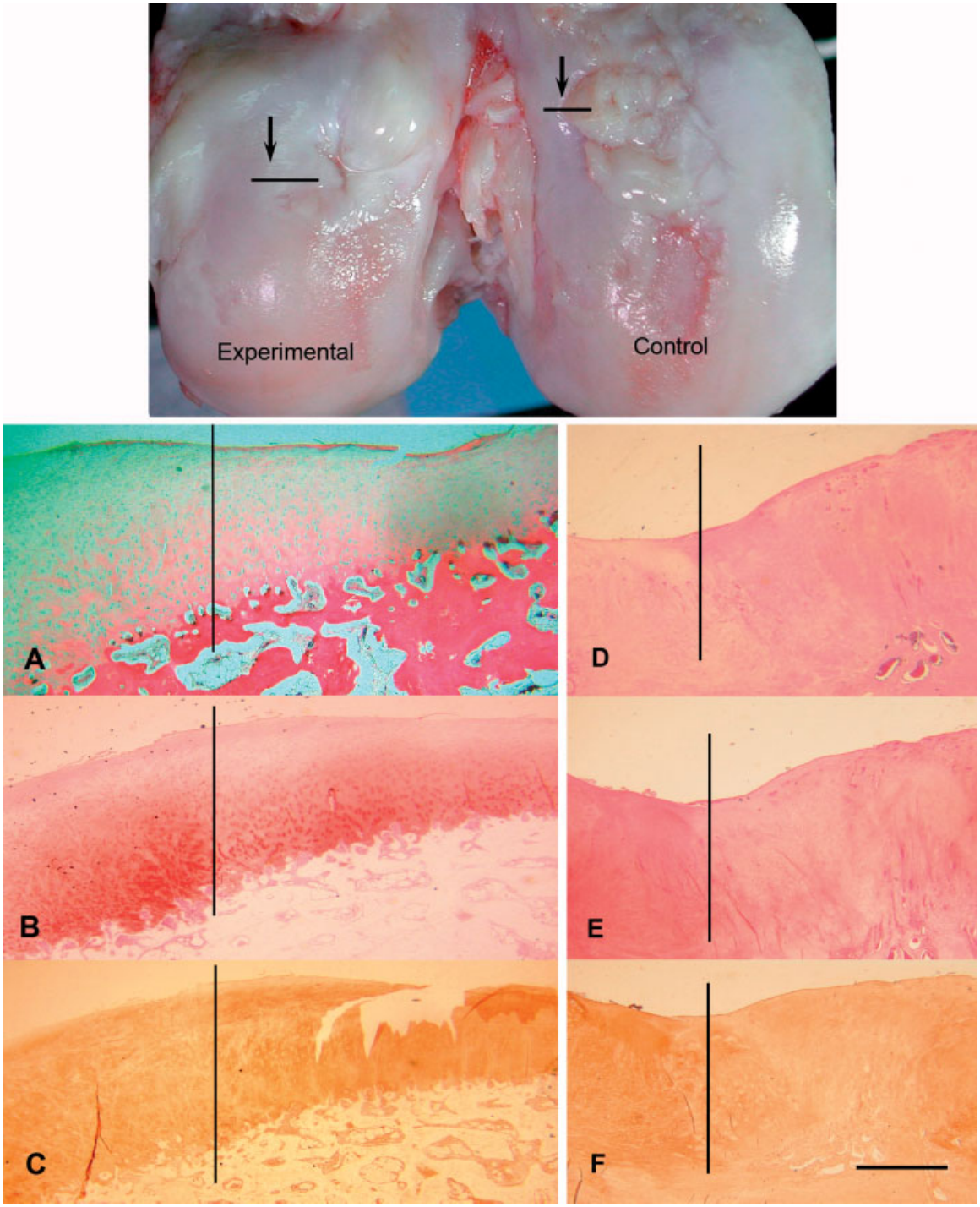

Figure 5. Histological and immunohistochemical analysis of regenerate cartilage. (Top) Gross view of animal #1, right knee, with arrow indicating the junction of repair and native tissues, and sections made at the indicated bar. (A, D) H&E staining; (B, E) Safranin O staining; and (C, F) immunohistochemical staining for collagen type II. Vertical lines indicate the borders of the repaired tissue, located to the right of the lines. (A–C) The lateral condyle of the experimental group: The regenerate cartilage was thinner than the adjacent native cartilage, yet contained sGAG (red Safranin O stain) and collagen type II (brown immunostain), with homogeneous ground substance (without dark H&E -stained fibrous streaks). (D–F) The medial condyle of control group had thick, soft regenerated tissue that was fibrous upon H&E -staining, and stained negatively for sGAG and collagen type II. (Bar = 1 mm).

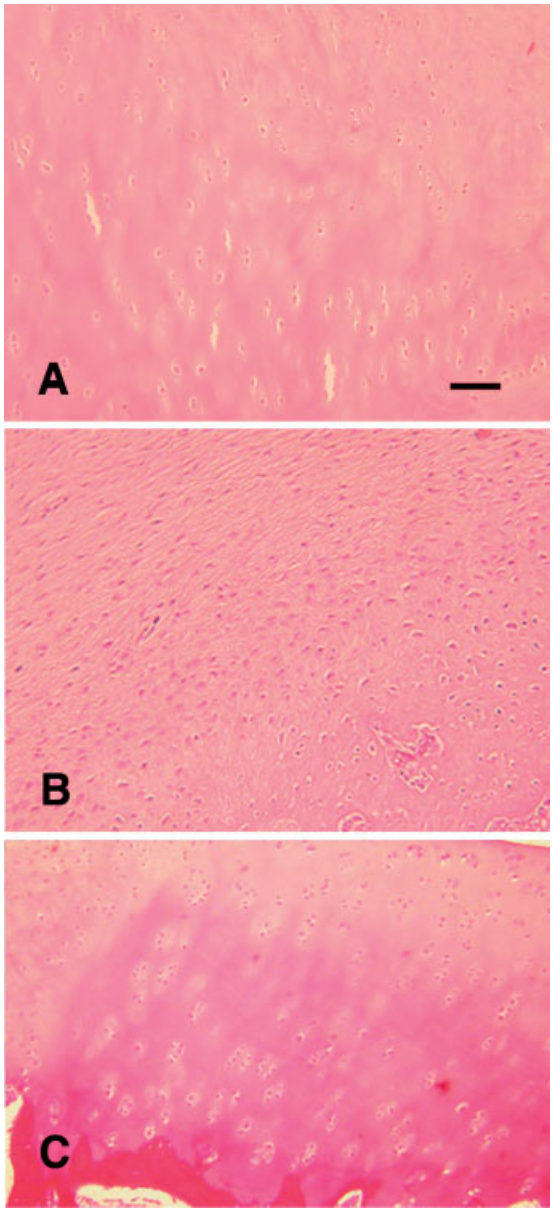

Figure 6. Higher magnification histology (H&E staining) of regenerate tissues in the chondral phase. (A) Experimental group—homogeneously distributed lacunated cells existed individually or in short column. (B) Control group—cells were predominantly spindle-shaped and resembled fibroblasts. (C) Native cartilage adjacent to the repaired site—typical nonhomogeneous cell distribution with palisade pattern near the osteochondral junction. (Bar = 100 μm).

within the chondral phase existed in 13 (of 18) specimens of the control group, and 11 (of 20) specimens of the experimental group.

Osseous Phase

Histologically, residual biomaterial was consistently present in the osseous phase of every repaired defect at 6 months, confirming that the construct did not dislodge from the recipient sites during the course of study (Fig. 7). Cells populated in the osseous phase of every repaired site, with generation of callus. New bone formed and partially replaced the biomaterial from the periphery, and the repair tissue seamlessly integrated with the native bone with microinterdigitation instead of a clear liner interface. However, normal architecture of cancellous bone had not been achieved completely to replace the biomaterial. In the experimental group, cancellous bone regenerated under the regenerate cartilage and fused with the cartilage with a clear tidemark as originally defined by the construct design.

X-ray roentgenography delineated a cystic radiolucent area larger than the originally cylindrical repair area, indicating that the cancellous bone adjacent to the implanted biomaterial underwent a remodeling process (Fig. 8).

Tissue Interface

In the experimental group, the osseous and chondral tissues regenerated separately in the corresponding phases of the biphasic constructs. Regardless of the nature of the regenerate cartilage, the tissues of the two phases of the construct adhered tightly with a clear tidemark that aligned with the native osteochondral junction. In the control group, the chondral phase was either replaced with fibrous tissue, or was devoid of regenerate tissue, thus exposing the underlying osseous part to the joint to give the original defect the appearance of a shallow pit with bony floor.

The regenerate cartilage was distinguishable histologically from native cartilage in most specimens. The integration between the regenerate cartilage and native cartilage was inconsistent and varied greatly even in a given specimen. In some areas, the two tissues were integrated with a transitional zone, where the surface was smoothly continuous without a step or notch. In other cases, the two tissues did not integrate and were separated by a gap. However, as described above, the osseous phase of the repaired tissue consistently integrated seamlessly with the native bone.

Mechanical Properties

At 30% strain, specimens of the experimental group ($n = 4$) and native cartilage ($n = 4$) showed similar biphasic stress–relaxation patterns. A peak stress was derived rapidly in the initial 6–13 s, to the average of 3.77 MPa for the experimental group and 5.17 MPa for the native

 DOI 10.1002/jor

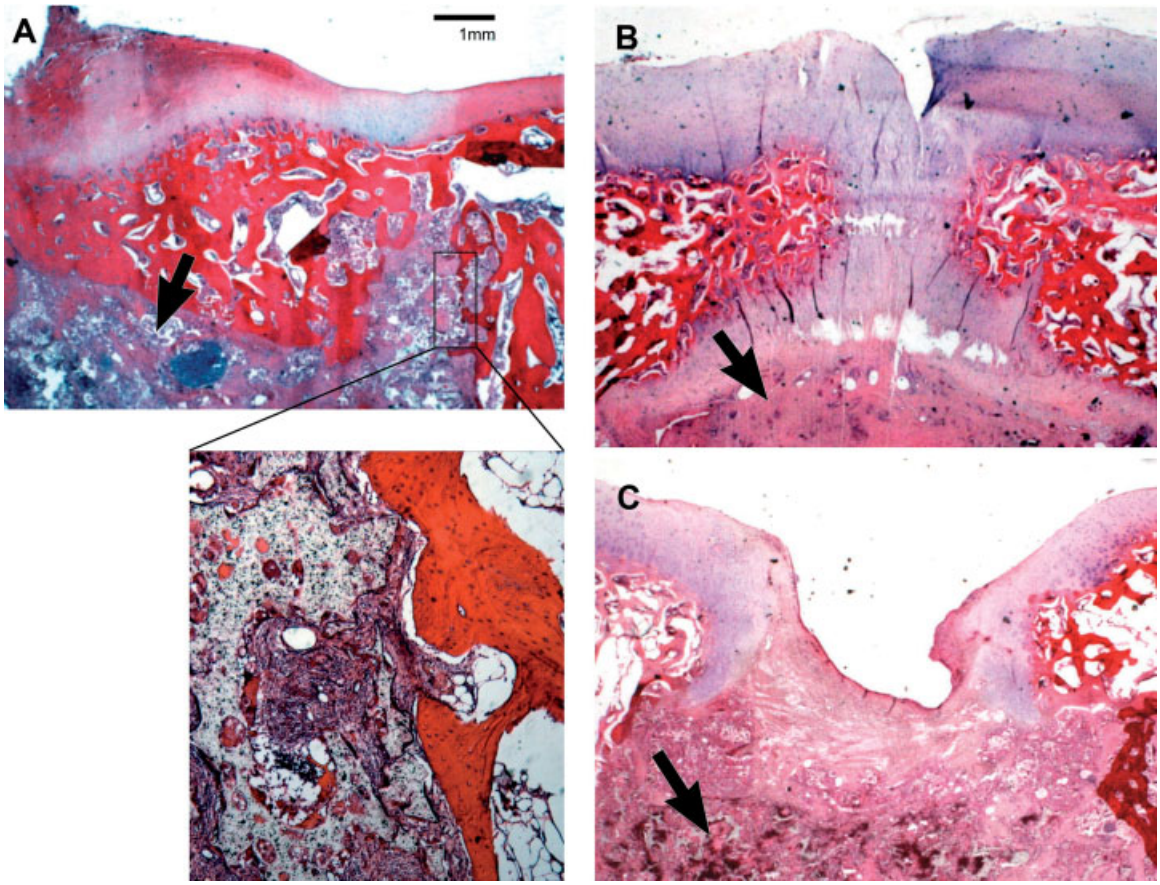

Figure 7. Histology of femoral condyles 6 months after implantation of biphasic construct (H&E staining), showing various patterns of cartilage regeneration. The biomaterial in the osseous phase of repaired sites was consistently present (arrows). (A) Experimental group, with well-established osteochondral tidemark. Regional magnification showing micro-integration between residual biomaterial and adjacent cancellous bone. Cells populated in the biomaterial, where scattered islets of ossification also formed. (B) Experimental group, with incomplete establishment of tidemark. Fissure formed on the joint surface, and was filled with fibrocartilaginous tissue. (C) Control group, where the repaired site remained indented, and the biomaterial of the osseous phase was covered with a fibrous top. [Bar = 1 mm; regional magnification of (A), 10×].

cartilage, representing the viscoelastic stiffness of these specimens. The stress peak was followed by a gradual decay to a final equilibrium in the next 30 min. The mean stress values from 20 to 30 min, the equilibrium stress that represented the time-independent tensile modulus of the solid phase in the viscoelastic material, were 0.93 and 0.88 MPa in these two respective groups.

The control group specimens ($n = 4$) behaved very differently under the same condition. The average maximal stress of 3.16 MPa was reached 20–36 s after the application of strain, and only dropped insignificantly thereafter. The equilibrium stress was 2.82 MPa, only slightly lower than the peak stress. An example of the stress changes with time is shown in Figure 9. This property indicated a rigid rather than viscoelastic material.

DISCUSSION

This study was designed to test the possibility of repairing osteochondral defects with relatively small number of chondrocytes transplanted with a biphasic construct. Cartilage regeneration with ACI is a time-consuming process and requires a minimum of 3 months to develop satisfactory repair tissue, with better repair expected by 6 months.[30–32] The intent of our study was to test the end result of cartilage repair, and thus only the 6-month timepoint was examined, without other shorter-term observations.

When repairing an osteochondral defect, subchondral cancellous bone formation is considered independent of the pre-seeding the construct with osteogenic cells.[33] The spongy construct would absorb the oozing marrow from the host cancellous

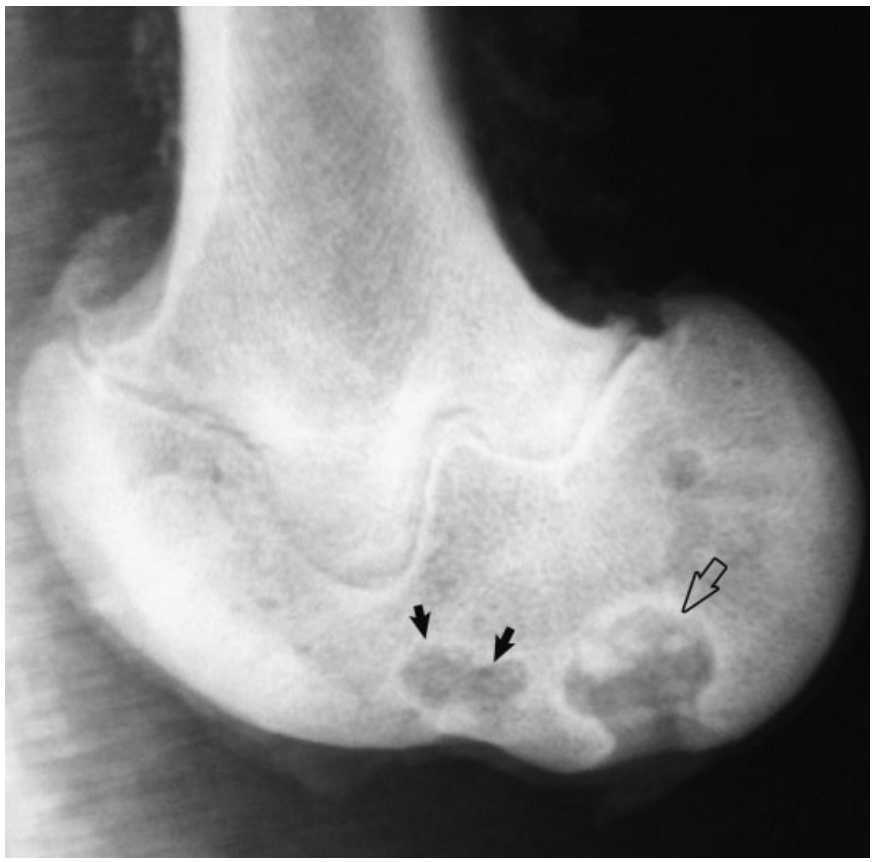

Figure 8. Plain X-ray roentgenography showing a subchondral cystic pouch of radiolucency (arrows), indicating remodeling within this area that included the implanted space and surrounding native tissue. Example shown here is the right knee of animal #9. (Solid arrows = lateral condyle, experimental group; open arrow = medial condyle, control group).

bone at the graft site. The osteogenic stromal cells in marrow can undergo osteogenesis when exposed to the TCP content of the construct, and build bony replacement while PLGA degrades.[34–36] Although many designs of osteochondral constructs have included pre-seeding of cells to build the osseous phase,[16,21,37] this is unnecessary for intraarticular application.[38] We observed bone formation in the osseous phase of all specimens, with evident subchondral remodeling. We did not determine whether such remodeling originated from the trauma of graft site preparation, or from chemical osteolysis by the acidic degradation product of PLGA. The remodeling may invade the osteochondral junction, resulting in formation of mineral buds/islands and capillary vessels in the regenerate cartilage, which should be normally avascular. However, a previous in vitro report about a similar biphasic construct, with PLGA/TCP in the osseous phase, indicates that the seeded chondrocytes preferentially stays in the chondral phase of PLGA.[23] This has held true in our observations.

A distinct advantage of the ACI procedure is the utilization of chondrocytes that produce appropriate ECM to replace the cartilage defect. Because chondrocytes have limited motility in vitro,[39–41] it is reasonable to assume that the native chondrocytes are unlikely to migrate a significant distance into the implanted biomaterial scaffold. We did not find such cells in the non-cell seeded scaffolds of the control group. A potential migratory cell population is the progenitor cells derived from bone marrow, although they most likely do not contribute to the generation of normal hyaline cartilage.[42] The fibroblast-like spindle cells we found in the chondral phase of control group might be derived from the marrow progenitor cells, or other intraarticular cell sources, such as the inflammatory cells. The absence of chondrocytes in the control group would suggest that the neocartilage in the experimental group was generated by the seeded chondrocytes. Thus, cartilage regeneration in implanted biomaterial scaffolds depends on pre-seeding with chondrogenic cells, but not on local host cells per se. The hyaline characteristics of the ECM in the

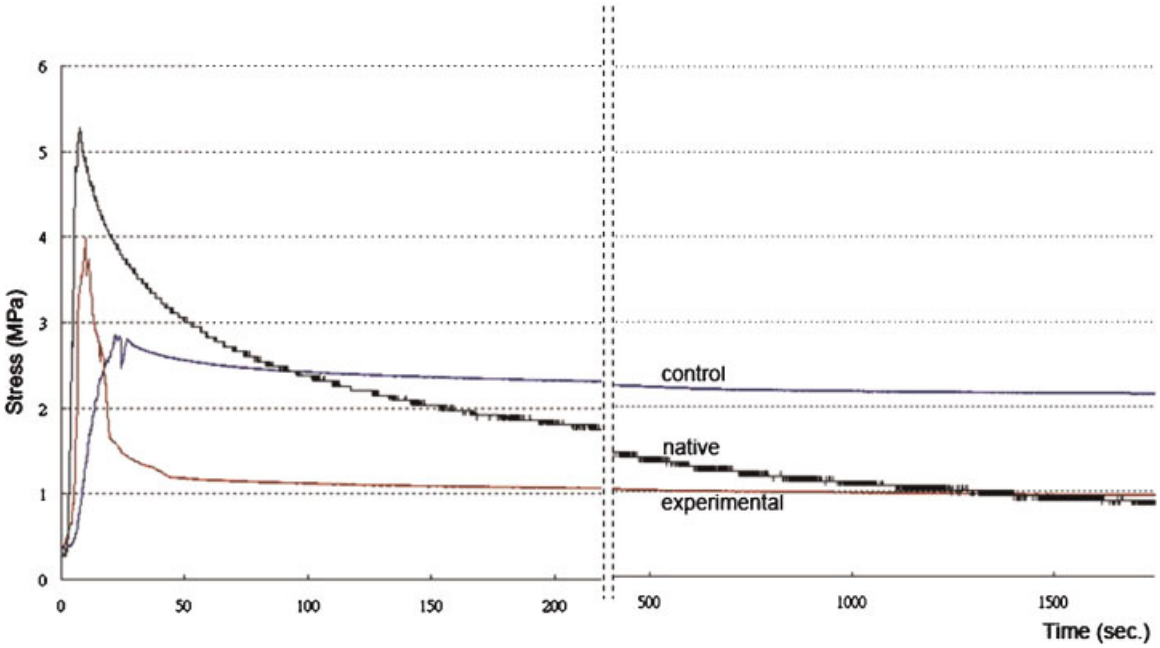

Figure 9. Mechanical property of specimens from left knee of animal #2 by indentation test at 30% of strain, showing the stress–relaxation process. The stresses of the experimental and native specimens rose in parallel to the peak values of 3.99 and 5.22 MPa at 10 and 7 s, respectively, then relaxed gradually to equilibrium values of 0.97 and 0.94 MPa, respectively, in the next 30 min. The stress of the control specimen rose more slowly, peaked at 24 s at 2.84 MPa, and dropped slightly to the equilibrium value of 2.16 MPa.

regenerate cartilage of the experimental group suggest that the seeded chondrocytes maintained their phenotype after being seeded in the biomaterial.

Cell-seeding density on biomaterial scaffold has been considered critical to the production of quality cartilage in tissue engineering. Densities as high as 10^7 cells/ml have been shown to elaborate abundant cartilage ECM.[17,43] However, more recent studies suggest that lower cell density, e.g., 10^4 cells/ml, can yield good cartilage identical to that from higher density, i.e., 10^6 cells/ml.[44] Excessive implanted cells may adversely affect the outcome of ACI by overgrowth of neocartilage to form a hump rising above the level of the native articular surface.[18] In principle, a lower but sufficient density of initially seeded cells, which then proliferate in the living joint and produce adequate ECM, may be optimal for cartilage regeneration.[18] The clinical relevance of our findings to ACI with lower cell density is the possibility of omitting the in vitro step of cell expansion, and combining cell harvest with implantation in the same surgery.

Various "semi-quantitative" scales have been used to qualify the regenerate cartilage.[45,46] Although with debatable validity, these scales provide objective reference parameters to compare cartilage samples.[47,48] The ICRS scale eliminates interobserver discrimination by a system of visual pattern parameters. Histologically, cartilage is classified as hyaline, elastic, or fibrous on the basis of the predominant substances in the ECM, which characterize the phenotype of chondrocytes, contribute to the mechanical characteristics of cartilage, and feedback regulate chondrocyte activities.[49] Although the Histological Endpoint Committee of ICRS recommends the sole use of H&E staining to evaluate cartilage, we believe that visualizing the content of ECM with special stains provides additional information to classify the regenerate cartilage. Because the nature and distribution of cells in a given specimen of regenerate cartilage usually showed regional variation, evaluation had to be based on the predominant pattern.

The ICRS scale includes cell distribution as a parameter to evaluate cartilage, because the lack of columnar distribution of chondrocytes in the middle and lower zones of cartilage indicates abnormal maturation.[20] The unique palisade pattern of uneven cell distribution in native articular cartilage is influenced by endochondral ossification of the epiphysis during bone maturation.[50] However, most models of ACI involve

uniform distribution of implanted cells in order to minimize local hypertrophy,[51] and this uniformity would be expected to be preserved in the regenerate cartilage. Although cartilage may undergo remodeling as a result of the mechanical stimulus of normal joint activity,[52,53] natural chondrocyte distribution was not seen in our study.

While the chondral phase of our constructs was completely replaced with regenerate tissue, substantial amount of biomaterials remained in the osseous phase 6 months after implantation. A previous animal study using TCP block to repair osteochondral defect reported 30%–50% resorption of the material at 8 weeks, and nearly complete resorption at 30 weeks.[38] Cell-based bioresorption of TCP was shown to be a slow process, with possible long-term persistence of this ceramic material. However, TCP has good osteoconductivity when used as a filler in the biomaterial implant, and may enhance the affinity of such implanted composite with bone.[54,55] Our observations are in agreement with these findings.

The mechanical characteristics of articular cartilage are difficult to define, and are influenced by many confounding factors, such as its anatomical location, the models of testing, and specific conditions of the joint.[29,56] The unconfined compression model has been shown to demonstrate the mechanical property of cartilage under physiological conditions.[57,58] One example of this model is the indentation creep test, which examines the overall response of cartilage under stress.[59] We used it to analyze the relative stress responses of cartilage specimens from the same joint, instead of calculating specific mechanical parameters. Both the experimental specimen and the native cartilage showed a similar creep response. Immediately after the peak stress, fluid was extruded from the material. The faster decay of stress indicated a faster loss of the fluid content, suggesting an inferior ability of material to trap fluid, or higher permeability. Stress at equilibrium reflected the support derived from the solid matrix of the material. In this respect, the experimental specimen lost its fluid content more quickly than native cartilage, yet eventually reached a similar equilibrium stress with the latter, meaning a similar stiffness of their solid content. The non-cell seeded control group depicted little creep effect under stress, consistent with a solid material or limited amount of interstitial fluid.

In conclusion, our findings indicate that using a single surgery procedure, the biphasic cylindrical construct, loaded with as many as 3×10^6 autogenous chondrocytes per milliliter, supports the regeneration of articular cartilage in vivo. The construct could be securely installed by press-fit without additional fixation. Cancellous bone forms in the osseous phase without pre-seeding of cells, and can integrate with the native subchondral bone. This approach presents an alternative to mosaicplasty, without the problems of insufficient graft resource and donor site morbidity, and the advantage of performing graft harvest and implantation in a single surgery.

ACKNOWLEDGMENTS

This work was supported in part by the Industrial Technology Research Institute (ITRI-IR91-1003), the National Taiwan University Hospital (NTUH-92A07), and the Intramural Research Program of NIAMS, NIH (AR ZO1 41131).

REFERENCES

1. Strauss EJ, Goodrich LR, Chen CT, et al. 2005. Biochemical and biomechanical properties of lesion and adjacent articular cartilage after chondral defect repair in an equine model. Am J Sports Med 33:1647–1653.
2. Frenkel SR, Bradica G, Brekke JH, et al. 2005. Regeneration of articular cartilage—evaluation of osteochondral defect repair in the rabbit using multiphasic implants. Osteoarthritis Cartilage 13:798–807.
3. Brittberg M, Lindahl A, Nilsson A, et al. 1994. Treatment of deep cartilage defects in the knee with autologous chondrocyte transplantation. N Engl J Med 331:889–895.
4. Grande DA, Pitman MI, Peterson L, et al. 1989. The repair of experimentally produced defects in rabbit articular cartilage by autologous chondrocyte transplantation. J Orthop Res 7:208–218.
5. Chiang H, Kuo TF, Tsai CC, et al. 2005. Repair of porcine articular cartilage defect with autologous chondrocyte transplantation. J Orthop Res 23:584–593.
6. Grigolo B, Roseti L, Fiorini M, et al. 2001. Transplantation of chondrocytes on a hyaluronan derivative (Hyaff-11) into cartilage defects in rabbits. Biomaterials 22:2417–2424.
7. Liu Y, Chen F, Liu W, et al. 2002. Repairing large porcine full-thickness defects of articular cartilage using autologous chondrocyte-engineered cartilage. Tissue Eng 8:709–721.
8. Noth U, Tuli R, Osyczka AM, et al. 2002. In vitro engineered cartilage constructs produced by press-coating biodegradable polymer with human mesenchymal stem cells. Tissue Eng 8:131–144.
9. Ushida T, Furukawa K, Toita K, et al. 2002. Three-dimensional seeding of chondrocytes encapsulated in collagen gel into PLLA scaffolds. Cell Transplant 11:489–494.
10. Kon M. 1981. Cartilage formation from perichondrium in a weight-bearing joint: an experimental study. Eur Surg Res 13:387–396.
11. O'Driscoll SW, Keeley FW, Salter RB. 1986. The chondrogenic potential of free autogenous periosteal grafts for

biological resurfacing of major full-thickness defects in joint surfaces under the influence of continuous passive motion: an experimental investigation in the rabbit. J Bone Joint Surg [Am] 68:1017–1035.
12. Giannini S, Vannini F, Buda R. 2002. Osteoarticular grafts in the treatment of OCD of the talus: mosaicplasty versus autologous chondrocyte transplantation. Foot Ankle Clin 7:621–633.
13. Hangody L, Feczko P, Bartha L, et al. 2001. Mosaicplasty for the treatment of articular defects of the knee and ankle. Clin Orthop 391 (Suppl):S328–S336.
14. Hangody L, Fules P., 2003. Autologous osteochondral mosaicplasty for the treatment of full-thickness defects of the weight-bearing joints: ten years of experimental and clinical experience. J Bone Joint Surg [Am] 85 (Suppl 2): 25–32.
15. Horas U, Pelinkovic D, Herr G, et al. 1985. Autologous chondrocyte implantation and osteochondral cylinder transplantation in cartilage repair of the knee joint. J Bone Joint Surg [Am] 85:185–192.
16. Schek RM, Taboas JM, Segvich SJ, et al. 2004. Engineered osteochondral grafts using biphasic composite solid free-form fabricated scaffolds. Tissue Eng 10:1376–1385.
17. Mauck RL, Seyhan SL, Ateshian GA, et al. 2002. Influence of seeding density and dynamic deformation loading on the developing structure/function relationships of chondrocyte-seeded agarose hydrogels. Ann Biomed Eng 30: 1046–1056.
18. Chaipinyo K, Oakes BW, van Damme M-PI. 2004. The use of debrided human articular cartilage for autologous chondrocyte implantation: maintenance of chondrocyte differentiation and proliferation in type I collagen gels. J Orthop Res 22:446–455.
19. Brittberg M. 1999. Autologous chondrocyte transplantation. Clin Orthop 367:S147–S155.
20. Mainil-Varlet P, Aigner T, Brittberg M, et al. 2003. Histological assessment of cartilage repair: a report by the Histology Endpoint Committee of the International Cartilage Repair Society (ICRS). J Bone Joint Surg [Am] 85 (Suppl 2):45–57.
21. Gao J, Dennis JE, Solchaga LA, et al. 2001. Tissue-engineered fabrication of an osteochondral composite graft using rat bone marrow-derived mesenchymal stem cells. Tissue Eng 7:363–371.
22. Schaefer D, Martin I, Shastri P, et al. 2000. In vitro generation of osteochondral composites. Biomaterials 21: 2599–2606.
23. Sherwood JK, Riley SL, Palazzolo R, et al. 2002. A three-dimensional osteochondral composite scaffold for articular cartilage repair. Biomaterials 23:4739–4751.
24. Tuli R, Nandi S, Li W-J. et al. 2004. Human mesenchymal progenitor cell-based tissue engineering of a single-unit osteochondral construct. Tissue Eng 10:1169–1179.
25. Wang X, Grogan SP, Rieser F, et al. 2004. Tissue engineering of biphasic cartilage constructs using various biodegradable scaffolds: an in vitro study. Biomaterials 25:3681–3688.
26. Liao CJ, Chen CF, Chen JH, et al. 2002. Fabrication of porous biodegradable polymer scaffolds using a solvent merging/particulate leaching method. J Biomed Mater Res 59:676–681.
27. Wayne JS, McDowell CL, Shields KJ, et al. 2005. In vivo response of polylactic acid-alginate scaffolds and bone marrow-derived cells for cartilage tissue engineering. Tissue Eng 11:953–963.
28. Mak AF, Lai WM, Mow VC. 1987. Biphasic indentation of articular cartilage—I: theoretical analysis. J Biomech 20: 703–714.
29. Mow VC, Gibbs MC, Lai WM, et al. 1989. Biphasic indentation of articular cartilage—II: a numerical algorithm and an experimental study. J Biomech 22:853–861.
30. Caplan AI, Elyaderani M, Mochizuki Y, et al. 1997. Principles of cartilage repair and regeneration. Clin Ortho 342:254–269.
31. Fan H, Hu Y, Zhang C, et al. 2006. Cartilage regeneration using mesenchymal stem cells and a PLGA-gelatin/chondroitin/hyaluronate hybrid scaffold. Biomaterials 27: 4573–4580.
32. Han CW, Chu CR, Adachi N, et al. 2003. Analysis of rabbit articular cartilage repair after chondrocyte implantation using optical coherence tomography. Osteoarthritis Cartilage 11:111–121.
33. Schaefer D, Martin I, Jundt G, et al. 2002. Tissue-engineered composites for the repair of large osteochondral defects. Arthritis Rheum 46:2524–2534.
34. Goshima J, Goldberg VM, Caplan AI. 1991. The origin of bone formed in composite grafts of porous calcium phosphate ceramic loaded with marrow cells. Clin Orthop 269:274–283.
35. Mankani MH, Kuznetsov SA, Fowler B, et al. 2001. In vivo bone formation by human bone marrow stromal cells: effect of carrier particle size and shape. Biotechnol Bioeng 72: 96–107.
36. Ohgushi H, Goldberg VM, Caplan AI. 1989. Heterotopic osteogenesis in porous ceramics induced by marrow cells. J Orthop Res 7:568–578.
37. Cao T, Ho KH, Teoh SH. 2003. Scaffold design and in vitro study of osteochondral coculture in a three-dimensional porous polycaprolactone scaffold fabricated by fused deposition modeling. Tissue Eng 9 (Suppl 1):S103–S112.
38. Tanaka T, Komaki H, Chazono M, et al. 2005. Use of a biphasic graft constructed with chondrocytes overlying a beta-tricalcium phosphate block in the treatment of rabbit osteochondral defects. Tissue Eng 11:331–339.
39. Chang C, Lauffenburger DA, Morales TI. 2003. Motile chondrocytes from newborn calf: migration properties and synthesis of collagen II. Osteoarthritis Cartilage 11:603–612.
40. Maniwa S, Ochi M, Motomura T, et al. 2001. Effects of hyaluronic acid and basic fibroblast growth factor on motility of chondrocytes and synovial cells in culture. Acta Orthop Scand 72:299–303.
41. Shimizu M, Minakuchi K, Kaji S, et al. 1997. Chondrocyte migration to fibronectin, type I collagen, and type II collagen. Cell Struct Funct 22:309–315.
42. Robinson D, Nevo Z. 2001. Articular cartilage chondrocytes are more advantageous for generating hyaline-like cartilage than mesenchymal cells isolated from microfracture repairs. Cell Tissue Bank 2:23–30.
43. Iwasa J, Ochi M, Uchio Y, et al. 2003. Effects of cell density on proliferation and matrix synthesis of chondrocytes embedded in atelocollagen gel. Artif Organs 27:249–255.
44. Willers C, Chen J, Wood D, et al. 2005. Autologous chondrocyte implantation with collagen bioscaffold for the treatment of osteochondral defects in rabbits. Tissue Eng 11:1065–1076.
45. Mankin HJ, Dorfman H, Lippiello L, et al. 1971. Biochemical and metabolic abnormalities in articular cartilage from osteo-arthritic human hips: II: correlation of morphology

with biochemical and metabolic data. J Bone Joint Surg [Am] 53:523–537.
46. O'Driscoll SW, Keeley FW, Salter RB. 1988. Durability of regenerated articular cartilage produced by free autogenous periosteal grafts in major full-thickness defects in joint surfaces under the influence of continuous passive motion: a follow-up report at one year. J Bone Joint Surg [Am] 70:595–606.
47. Ostergaard K, Petersen J, Andersen CB, et al. 1997. Histologic/histochemical grading system for osteoarthritic articular cartilage: reproducibility and validity. Arthritis Rheum 40:1766–1771.
48. van der Sluijs JA, Geesink RG, van der Linden AJ, et al. 1992. The reliability of the Mankin score for osteoarthritis. J Orthop Res 10:58–61.
49. van der Kraan PM, Buma P, van Kuppevelt T, et al. 2002. Interaction of chondrocytes, extracellular matrix and growth factors: relevance for articular cartilage tissue engineering. Osteoarthritis Cartilage 10:631–637.
50. Glimore RSC, Palfrey AJ. 1988. Chondrocyte distribution in the articular cartilage of human femoral condyles. J Anat 157:23–31.
51. Sohn DH, Lottman LM, Lum LY, et al. 2002. Effect of gravity on localization of chondrocytes implanted in cartilage defects. Clin Ortho 394:254–262.
52. Shen G, Darendeliler MA., 2005. The adaptive remodeling of condylar cartilage: a transition from chondrogenesis to osteogenesis. J Dent Res 84:691–699.
53. Trumble T, Verheyden J. 2004. Remodeling of articular defects in an animal model. Clin Ortho 423: 59–63.
54. Arnold U, Lindenhayn K, Perka C. 2002. In vitro-cultivation of human periosteum derived cells in bioresorbable polymer-TCP-composites. Biomaterials 23: 2303–2310.
55. Goto K, Shinzato S, Fujibayashi S, et al. 2006. The biocompatibility and osteoconductivity of a cement containing beta-TCP for use in vertebroplasty. J Biomed Mater Res A 78:629–637.
56. Elliott DM, Guilak F, Vail TP, et al. 1999. Tensile properties of articular cartilage are altered by menisectomy in a canine model of osteoarthritis. J Orthop Res 17: 503–508.
57. Altman RD, Tenenbaum J, Latta L, et al. 1984. Biomechanical and biochemical properties of dog cartilage in experimentally induced osteoarthritis. Ann Rheum Dis 43:83–90.
58. Coletti JM Jr, Akeson WH, Woo SL. 1972. A comparison of the physical behavior of normal articular cartilage and the arthroplasty surface. J Bone Joint Surg [Am] 54:147–160.
59. Mow VC, Gu WY, Chen FH. 2005. Structure and function of articular cartilage and meniscus. In: Mow VC, Huiskes R, editors. Basic orthopaedic biomechanics and mechanobiology, 3rd ed. Philadelphia: Lippincott Williams & Wilkins. pp 181–258.